GEOPHYSICAL RESEARCH LETTERS, VOL. 40, 1–5, doi:10.1002/grl.50759, 2013

A reduced complexity model for dynamic similarity in obstructed shear flows

A. Papke[1,2] and I. Battiato[1]

Received 31 May 2013; revised 10 July 2013; accepted 12 July 2013.

[1] Coupled flows through and over permeable media, also known as obstructed shear flows, are ubiquitous to many environmental systems at different scales, including aquatic flows over sediment beds, and atmospheric flows over crops and cities. Despite their differences, such flows exhibit strong dynamic similarities among systems and scales, as evidenced by the recent finding of empirical universal scaling laws correlating relevant length and velocity scales. We propose a reduced complexity model for obstructed shear channel flows, which couples Brinkman with Reynolds equations to describe the flow within and above the obstruction. We derive scaling laws by intermediate asymptotic analysis of a Darcy-Brinkman type solution in the low permeability limit. The approach highlights the importance of the effective permeability of the obstruction as a critical parameter governing the system dynamical response. The model results are in good agreement with the scaling laws empirically calculated in other studies. **Citation:** Papke, A., and I. Battiato (2013), A reduced complexity model for dynamic similarity in obstructed shear flows, *Geophys. Res. Lett.*, *40*, doi:10.1002/grl.50759.

1. Introduction

[2] Coupled flows through and over permeable media, also referred to as "obstructed shear flows" [*Ghisalberti*, 2009], occur in a variety of environmental (and engineered) systems. In aquatic and terrestrial environments, some examples include laminar or turbulent flows over sediment beds, submerged vegetation, coral reefs, forests, crop canopies, and cities.

[3] The dynamics of the flow at the interface between the obstruction and the free fluid is critical in determining mass, heat, and momentum transfer between the two regions. For example, wind-plant interactions determine thermal convection and seed dispersion [*de Langre*, 2008], together with carbon dioxide and energy exchange between canopies and the atmosphere [*Baldocchi and Meyers*, 1998]; in aquatic ecosystems, vegetation influences temperature of the environment and the supply of light, oxygen, carbon, and nutrients [*Carpenter and Lodge*, 1986]. We refer to, e.g., *Nepf* [2012], *de Langre* [2008], and *Finnigan* [2000] for reviews on terrestrial and aquatic canopy flows.

[4] A common feature to many obstructed shear flows is the experimental evidence of Kelvin-Helmholtz (KH) type vortices generated by an inflection point in the mean velocity profile. Similar coherent structures have been observed in boundary-layer flows adjacent to a range of porous [*Jiménez et al.*, 2001; *Shvidchenko and Pender*, 2001] and roughness layers, e.g., grooves or spanwise cylinders. Numerical simulations revealed that turbulent channel flows over sediment (i.e., packed) beds are dominated by a KH type of instability as well [*Breugem et al.*, 2006]. Other types of obstructed shear flows, such as flows over coral reefs and urban canopies, exhibit an inflection point in the mean velocity profile while little evidence of coherent structures exists.

[5] It has been suggested that coherent vortical structures generated by a shear instability may be a common feature of flows over rough or permeable media [*White and Nepf*, 2007]. Evidence of such dynamical similarity for a range of environmental flows is provided in *Ghisalberti* [2009], where scaling laws are empirically developed from a set of data, spanning systems from the millimeter to the meter scale. Both laboratory and field data of flows over submerged aquatic vegetation canopies, terrestrial vegetation canopies, coral reefs, dense porous media, and experimental flows adjacent to vegetation were considered [*Ghisalberti*, 2009, and references therein]. Such laws relate relevant length and velocity scales to each other, e.g., the extent of the shear penetration into the obstruction with the drag length scale, and the slip velocity to the friction velocity.

[6] In this letter, we propose a reduced complexity semiempirical model for obstructed shear flows, which treats the obstruction as a porous medium and couples Brinkman with Reynolds equations to describe the flow within and above the obstruction. This allows us (i) to derive analytical solutions for the mean velocity and stress profiles within the obstruction and (ii) to establish self-similarity of coupled flows inside and over permeable layers as intermediate asymptotics in the low permeability limit. The previous results, combined with the experimental observation that the canopy shear layer parameter is statistically constant, lead to scaling laws in good agreement with those empirically identified by *Ghisalberti* [2009].

2. Reduced Complexity Model

[7] We consider a fully developed incompressible fluid flow in a two-dimensional channel formed by two impermeable walls at a mutual distance of $H + 2L$. The bottom part of the channel, $\hat{y} \in (-H, 0)$, is occupied by an array of obstacles (aquatic or terrestrial vegetation, urban canopies, etc.) which we model as a porous medium with permeability K (see Figure 1). The flow is driven by an imposed mean

[1]Department of Mechanical Engineering, Clemson University, Clemson, South Carolina, USA.
[2]Max Planck Institute for Dynamics and Self-Organization, Göttingen, Germany.

Corresponding author: I. Battiato, Department of Mechanical Engineering, Clemson University, 233 Fluor Daniel Building, Clemson, SC 29634, USA. (ibattia@clemson.edu)

©2013. American Geophysical Union. All Rights Reserved.
0094-8276/13/10.1002/grl.50759

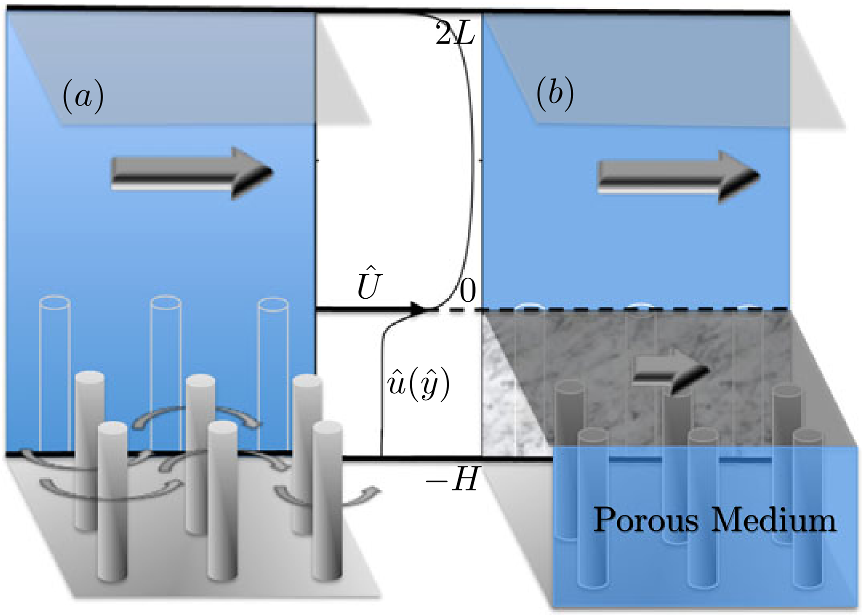

Figure 1. (a) Schematics of channel flow through $\hat{y} \in [-H, 0]$ and above $\hat{y} \in (0, 2L]$, a forest of cylindrical obstacles. (b) Effective medium representation of the obstruction. The solid line represents the (spatial) mean velocity profile, $\hat{u}(\hat{y})$ inside and above the porous medium, and $\hat{U}$ is the velocity coupling the porous medium with the free flow at the fictitious interface (dashed line).

pressure gradient $\mathrm{d}_{\hat{x}}\hat{p} < 0$. We use steady state Reynolds equations to describe fully developed turbulent flow over the porous layer, $\hat{y} \in (0, 2L)$,

$$\mu \mathrm{d}_{\hat{y}\hat{y}}\hat{u} - \rho\, \mathrm{d}_{\hat{y}}\langle \hat{u}'\hat{v}' \rangle - \mathrm{d}_{\hat{x}}\hat{p} = 0, \qquad \hat{y} \in (0, 2L), \qquad (1)$$

where ρ and μ are the fluid density and dynamic viscosity, $\hat{\mathbf{u}} = [\hat{u}, \hat{v}]$ denotes the mean velocity, $\hat{u}'$ and $\hat{v}'$ are the velocity fluctuations about their respective means, and $\langle \hat{u}'\hat{v}' \rangle$ is the Reynolds stress. Fully developed turbulent channel flow has velocity statistics that depend on $\hat{y}$ only. Equation (1) can be closed by employing the turbulent viscosity hypothesis,

$$\langle \hat{u}'\hat{v}' \rangle = -\nu_t(\hat{y})\mathrm{d}_{\hat{y}}\hat{u}, \qquad (2)$$

where ν_t is the eddy viscosity. The eddy viscosity closure assumption has been successfully employed to model obstructed shear flows elsewhere [*Ghisalberti and Nepf*, 2004, equation (5)], and it is therefore deemed reasonable. Combining (2) with (1), we obtain

$$\mathrm{d}_{\hat{y}}\hat{\tau}(\hat{y}) - \mathrm{d}_{\hat{x}}\hat{p} = 0, \qquad \hat{y} \in (0, 2L), \qquad (3)$$

where $\hat{\tau}(\hat{y}) = \mu_T(\hat{y})\mathrm{d}_{\hat{y}}\hat{u}$, $\mu_T(\hat{y}) = \mu + \mu_t(\hat{y})$, and $\mu_t = \rho\nu_t$. Integrating (3) from $\hat{y}=0^+$ to $\hat{y}=L$, while assuming that $\hat{\tau}(L) \approx 0$, we obtain

$$\hat{\tau}(0^+) = \mu_T(0^+)\mathrm{d}_{\hat{y}}\hat{u}|_{0^+} \approx -L\mathrm{d}_{\hat{x}}\hat{p}, \qquad (4)$$

which provides a condition for the stress at the interface between free and filtration flows. The former assumption is not strictly valid since the flow is not perfectly symmetric about $\hat{y}=L$ due to a nonzero velocity $\hat{U}$ at the interface between the channel and the porous medium. However, $\hat{\tau}(L) \approx 0$ represents an increasingly better approximation as the permeability of the obstruction (and $\hat{U}$) decreases.

[8] The flow through the porous medium region, $\hat{y}=(-H, 0)$, can be described by Brinkman equation for the horizontal component of the intrinsic velocity $\hat{u}(\hat{y})$ [*Hsieh and Shiu*, 2006; *Battiato et al.*, 2010; *Battiato*, 2012],

$$\mu_e\, \mathrm{d}_{\hat{y}\hat{y}}\hat{u} - \mu_e K^{-1}\hat{u} - \mathrm{d}_{\hat{x}}\hat{p} = 0, \qquad \hat{y} \in (-H, 0), \qquad (5)$$

where the effective viscosity μ_e is a fitting parameter that arises from homogenization techniques [*Auriault*, 2009], and K is the porous medium permeability. While the latter can vary with $\hat{y}$, we treat it as constant throughout the porous medium. Guided by experimental evidence [e.g., *Ghisalberti and Nepf*, 2004; *White and Nepf*, 2007; *Poggi et al.*, 2009; *Katul et al.*, 2011], we impose a no-shear condition at $\hat{y}=-H$, and the continuity of velocity and shear stress at the interface, $\hat{y}=0$, between the free and obstructed flows:

$$\mathrm{d}_{\hat{y}}\hat{u}(-H) = 0, \quad \hat{u}(0^-) = \hat{U}, \quad \mu_e \mathrm{d}_{\hat{y}}\hat{u}|_{0^-} = \mu_T(0^+)\mathrm{d}_{\hat{y}}\hat{u}|_{0^+}, \qquad (6)$$

where $\hat{U}$ is an unknown velocity at the interface. Experimental measurements of obstructed shear flows exhibit smooth mean velocity profiles across the interface separating the vegetated layer from the free flow. Therefore, we set $\mu_e := \mu + \mu_t(0^+)$ in equations (5) and (6). For $|\hat{y}| < \mathcal{O}(K^{1/2})$, the Brinkman term in equation (5) is negligible, and a Darcian mean velocity profile, $\hat{U}_d = -K\mathrm{d}_{\hat{x}}\hat{p}/\mu_e$, is recovered.

[9] Choosing the height of the porous medium, H, the velocity $q = -H^2\mathrm{d}_{\hat{x}}\hat{p}/\mu_e$ and the fluid effective viscosity, μ_e, as repeating variables, equation (5) can be cast in dimensionless form,

$$\mathrm{d}_{yy}u - \lambda^2 u + 1 = 0, \quad y \in (-1, 0), \qquad (7)$$

subject to

$$\mathrm{d}_y u|_{-1} = 0, \quad u(0^-) = U, \quad \mathrm{d}_y u|_{0^-} = \delta, \qquad (8)$$

where $u = \hat{u}/q$, $U = \hat{U}/q$, and $\delta = L/H$. In (7), the parameter $\lambda^2 = H^2/K$ is inversely proportional to permeability.

The system (7)–(8) is amenable to an analytical solution for the dimensionless velocity distribution $u(y)$ inside the obstruction $y \in [-1, 0]$:

$$u(y) = \lambda^{-2} + C_1 e^{\lambda y} + C_2 e^{-\lambda y}, \quad (9a)$$

$$C_{1,2} = (U - \lambda^{-2} \pm \delta\lambda^{-1})/2, \quad (9b)$$

$$U = \lambda^{-2} + \delta\lambda^{-1} \coth \lambda. \quad (9c)$$

In (9), the dimensionless Darcy velocity is given by $U_d = \hat{U}_d/q = \lambda^{-2}$.

3. Quantities of Interest

[10] The dynamics of obstructed shear flows, and specifically of flows above canopies [*Ghisalberti*, 2009], is described by few characteristic velocity and length scales.

[11] The relevant velocity scales are the interfacial velocity, $\hat{U}$, the Darcy velocity deep in the obstruction, $\hat{U}_d$, and the friction velocity, $\hat{u}_\tau$, defined as

$$\hat{u}_\tau = \sqrt{\hat{\tau}(0)/\rho}. \quad (10)$$

[12] The penetration length, $\hat{\delta}_e$, represents the penetration distance of the vortices into the canopy and is defined as the distance from the interface, $\hat{y}=0$, where the stress has decayed to some fixed, however arbitrary, percentage of its maximum value measured at the interface, $\hat{\tau}_{\max} = \hat{\tau}(0)$. Often, such percentage is fixed at 10% of $\hat{\tau}_{\max}$ [*Nepf and Vivoni*, 2000; *Ghisalberti*, 2009], i.e.,

$$\hat{\delta}_e : \quad \hat{\tau}(-\hat{\delta}_e) = 0.10\hat{\tau}(0). \quad (11)$$

The length $\hat{\delta}_e$ is the primary scale determining the mean residence time within the obstruction and separates the canopy upper layer of rapid renewal from a lower layer of limited mixing rates [*Ghisalberti and Nepf*, 2005].

[13] Another important length scale, beside the obstruction height H, is the drag length scale, $\hat{b}$,

$$\hat{b} := \frac{1}{C_D a}, \quad (12)$$

where C_D and a are the drag coefficient of the medium and the frontal area of the obstructions per unit volume, respectively. The drag length scale is related to the canopy shear layer parameter, CSL, which is statistically constant across a wide range of experiments [*Nepf et al.*, 2007], i.e.,

$$\mathrm{CSL} := C_D a \frac{\hat{U}}{\mathrm{d}_{\hat{y}}\hat{u}|_0} \approx 0.23. \quad (13)$$

4. Self-Similarity in Obstructed Shear Flows

4.1. Data

[14] In his work, *Ghisalberti* [2009] identifies universal laws between relevant velocity and length scales, which strongly suggest the inherent dynamic similarity of a variety of obstructed shear flows on scales from $\mathcal{O}$(mm) to $\mathcal{O}$(10m). The author employs data from over 100 flows, including flows over submerged aquatic and terrestrial vegetation canopies, urban canopies (including pressure-driven wind tunnel experiments), coral reefs, and dense porous media, just to mention a few. Some of the restrictions to the selected data include the following: (i) obstructions with $C_D aH > 0.25$, i.e., the obstructions had to be sufficiently dense (i.e., low permeable) to induce an inflection point in the mean velocity profile; and (ii) flows with $C_D aL > 0.5$, i.e., flows where the upper boundary (e.g., free surface or the channel half height) does not limit the vortex growth. The collected data revealed the following scaling laws [*Ghisalberti*, 2009]:

$$\hat{\delta}_e \approx \frac{1}{3}\hat{b}, \quad (14a)$$

$$\hat{U} - \hat{U}_d \approx 2.6\hat{u}_\tau. \quad (14b)$$

Figures 2(a) and 2(b) (adapted from *Ghisalberti* [2009], Figures 4(a) and 4(b)) report data as collected by Ghisalberti, and the empirical scaling laws (14a) and (14b) (solid grey lines) with their 90% prediction interval (dashed lines), respectively.

4.2. Self-Similarity by Asymptotic Analysis

[15] Following *Battiato* [2012], we seek dynamic similarity by studying the asymptotic behavior of the solution (9) in the low permeability limit, i.e., $\lambda \to +\infty$. The notation $\lambda \to +\infty$ will be always implied whenever an asymptotic behavior is calculated.

[16] Since $\coth\lambda \sim 1$, we obtain

$$U \sim \frac{\Lambda + 1}{\lambda^2} \quad (15)$$

where $\Lambda = \delta\lambda$. Equation (15) exhibits two different limits depending on whether $\Lambda \gg 1$ or $\Lambda \ll 1$. The parameter Λ is a dimensionless number that compares the height of the free flow region to the transition zone thickness (the distance away from the interface $y=0$ where the velocity profile becomes Darcian). As in *Battiato* [2012], a classification between thin ($\Lambda \gg 1$) and thick ($\Lambda \ll 1$) porous media is employed. Unlike its counterparts based solely on geometrical ratios (e.g., $\delta \gg 1$ or $\delta \ll 1$), this definition engenders a dynamical classification. It depends on the medium permeability and may not be directly related to the physical dimensions of the porous layer. For example, a medium is classified as thin if, for a fixed height ratio δ, its dimensionless permeability is sufficiently low, i.e., $\lambda \gg \delta^{-1}$ (or $\Lambda \gg 1$). For thin and thick porous media, $U \sim \delta/\lambda$ and $U \sim \lambda^{-2}$, respectively. Combining (9c) with (9b), while observing that $\coth\lambda - 1 \sim 2e^{-2\lambda}$, we obtain

$$C_1 \sim \frac{\delta}{\lambda}, \quad (16a)$$

$$C_2 \sim \frac{\delta}{\lambda e^{2\lambda}}. \quad (16b)$$

Inserting (16) in (9a) leads to the following asymptotic behavior:

$$u^\star(y^\star; \lambda) := [u(y^\star/\lambda; \lambda) - U_d] \sim \delta\lambda^{-1} e^{y^\star}(1 + e^{-2y^\star - 2\lambda}), \quad (17)$$

where $y^\star = \lambda y$, with $y^\star \in [-\lambda, 0]$, and $u^\star$ are a rescaled coordinate and velocity, respectively. Since $-2y^\star - 2\lambda < 0$ for any $y^\star \in [-\lambda, 0]$, the exponentially decaying term in (17) can be neglected, and (17) can be further simplified to

$$u^\star(y^\star; \lambda) \sim \delta\lambda^{-1} e^{y^\star}, \quad y^\star \in [-\lambda, 0]. \quad (18)$$

Similarly, an asymptotic analysis of the dimensionless stress $\tau = \hat{\tau}H/(\mu_e q) = \mathrm{d}_y u$ gives

$$\tau(y^\star) \sim \delta e^{y^\star}, \quad y^\star \in [-\lambda, 0], \quad (19)$$

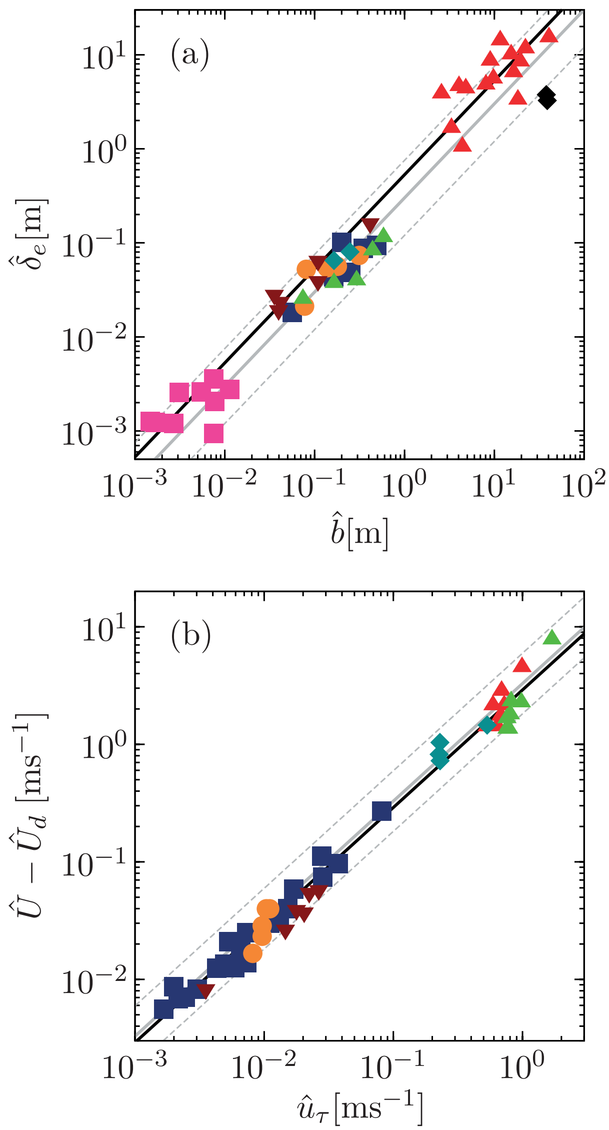

Figure 2. Empirical (solid grey lines) and calculated (solid black lines) scaling laws as given in (14a) (or (14b)) and (24) (or (30)), respectively. The dashed grey lines represent the 90% prediction interval associated with the empirical scaling laws (14a) and (14b). Data, reproduced from [*Ghisalberti*, 2009, and references therein], include several systems: experimental flows over rigid model aquatic vegetation (blue squares), coral reefs (orange circles), dense porous media (pink squares), waving model aquatic vegetation (brown inverted triangles), model terrestrial vegetation (green triangles), model urban canopies (cyan diamonds), real flows over terrestrial vegetation (red triangles), and urban canopies (black diamonds).

i.e., $\tau(y^\star)$ exhibits a self-similar behavior independent of medium permeability in the entire domain. Combining (11) with (19) evaluated at $y^\star=0$, we obtain

$$\lambda\delta_e \sim \ln 10 \tag{20}$$

with $\delta_e=\hat{\delta}_e/H$, the dimensionless penetration length. Equation (20) provides a scaling behavior for δ_e in the low permeability limit and shows that the penetration length is inversely proportional to λ (or directly proportional to permeability). Since $\mathrm{d}_y u=\tau$, casting (13) in dimensionless form, yields

$$\frac{C_D aHU}{\tau(0)} \approx 0.23. \tag{21}$$

Inserting (19) into (21), while accounting for the asymptotic behavior of U in thin porous media, leads to

$$\frac{C_D aH}{\lambda} \sim 0.23. \tag{22}$$

Equation (22), which provides a relationship between the drag length scale and permeability, allows one to a posteriori verify if the asymptotic analysis developed in the low permeability limit ($\lambda\to+\infty$) is a valid approximation for the data set investigated by *Ghisalberti* [2009]. The "dense" porous media condition, i.e., $C_D aH>0.25$, combined with (22), corresponds to $\mathcal{O}(\lambda)>1$, which is consistent with the asymptotic limit investigated here. Additionally, the condition $C_D aL>0.5$, when cast in terms of the dimensionless thickness δ, becomes $C_D aH>0.5/\delta$. Combining the latter with (22) leads to the bound $\Lambda>2.17$, which is consistent with the thin porous medium approximation ($\Lambda>1$). Combination of (20) and (22) leads to

$$\hat{\delta}_e C_D a \sim 0.23 \ln 10. \tag{23}$$

Alternatively, (23) can be rearranged as follows:

$$\hat{\delta}_e \approx 0.53\,\hat{b}, \tag{24}$$

which recovers the linear dependence between $\hat{\delta}_e$ and $\hat{b}$, as empirically observed in the scaling law (14a). Figure 2(a) shows the relationship between the penetration length $\hat{\delta}_e$ and the drag length scale $\hat{b}$ as described by (14a) (solid grey line) and (24) (solid black line). The scaling resulting from the proposed model as intermediate asymptotic of a Darcy-Brinkman-type solution in the low permeability limit well matches the empirical scaling proposed by *Ghisalberti* [2009].

[17] The drag coefficient is defined as $C_D=2|\hat{F}_D|/(\rho A_f \hat{U}_c^2)$ where $\hat{F}_D(\hat{y})$ is the drag force on array elements of total frontal area $A_f(\hat{y})$, and $\hat{U}_c$ is a representative fluid velocity. The former equation can be rewritten as

$$C_D a = \frac{2|\hat{F}|}{\rho \hat{U}_c^2} \tag{25}$$

where $\hat{F}$ is now the drag force per unit volume of porous medium. In a Brinkman medium, $\hat{F}=-\mu_e\hat{u}/K$ [*Guo et al.*, 2000]. At the interface, $\hat{F}(0^-)=-\mu_e\hat{U}/K$. The former equation can be recast in terms of dimensionless quantities as,

$$\hat{F}(0) = -\frac{\lambda^2 U}{H}\frac{\hat{\tau}(0)}{\tau(0)}, \tag{26}$$

since $\hat{\tau}/\tau=\mu_e q/H$ by definition of dimensionless stress. Inserting (26) in (25) while accounting for (10) leads to

$$C_D aH = 2\lambda^2 \frac{U}{\tau(0)}\left(\frac{\hat{u}_\tau}{\hat{U}_c}\right)^2. \tag{27}$$

In the low permeability limit and for thin porous media, (15) and (19) give $U\sim\delta/\lambda$ and $\tau(0)\sim\delta$, respectively. Therefore, (27) becomes

$$\left(\frac{\hat{u}_\tau}{\hat{U}_c}\right)^2 \sim \frac{1}{2}\frac{C_D aH}{\lambda}. \tag{28}$$

Inserting (22) in (28) gives

$$\hat{U}_c \sim 2.95\hat{u}_\tau. \quad (29)$$

A priori, the characteristic velocity $\hat{U}_c$ can be taken as $\hat{U}$, $\hat{U}_d$, or $\hat{U} - \hat{U}_d$ [*Ghisalberti*, 2009]. Choosing $\hat{U} - \hat{U}_d$ as characteristic velocity in (29) yields

$$\hat{U} - \hat{U}_d \sim 2.95\hat{u}_\tau. \quad (30)$$

We stress that the alternative choice $\hat{U}_c := \hat{U}$ would be still appropriate since both $\hat{U}$ and $\hat{U} - \hat{U}_d \,(= qu^\star(0))$, as defined in (17), exhibit the same asymptotic behavior as $\lambda \to +\infty$, $\hat{U}/q \sim u^\star(0) \sim \delta/\lambda$. On the contrary, based on the proposed model, the choice of $\hat{U}_d$ seems less appropriate since it has a different scaling, i.e., $\hat{U}_d/q \sim 1/\lambda^2$. Figure 2(b) plots the experimental data as in *Ghisalberti* [2009], and the scaling laws (14b) and (30) obtained by data fitting (solid grey line) and the proposed model (30) (solid black line), respectively. The model results are in good agreement with the experimental data.

5. Concluding Remarks

[18] It has been empirically showed that flows over permeable layers, alias obstructed shear flows, exhibit dynamic similarity across scales ranging from the millimeter to the meter, and in a plethora of environmental systems.

[19] We propose a reduced complexity model for turbulent flow over obstructions which treats the obstruction as a porous medium and employs a coupled system of Brinkman and Reynolds equations to analytically determine the mean velocity profile inside the porous medium. This approach highlights the critical importance of the effective permeability of the obstruction (as opposed to its porosity, as generally reported in other studies) on the dynamical behavior of the system.

[20] Asymptotic analysis of the solution in the low permeability limit allows one (i) to identify a critical scale parameter, Λ, to formally classify thin ($\Lambda \gg 1$) and thick ($\Lambda \ll 1$) porous media, and (ii) to analytically derive universal scaling laws relating characteristic length and velocity scales in obstructed shear flows.

[21] The predicted scaling laws derived from the proposed model well compare with the empirical ones calculated by *Ghisalberti* [2009]. Such agreement suggests that the proposed approach may be an appropriate framework for modeling shear flows over obstructions at a variety of scales.

[22] **Acknowledgments.** Ariane Papke gratefully acknowledges funding from Georg-August-Universität Göttingen and the Max Planck Institute for Dynamics and Self-Organization, Göttingen.

[23] The editor thanks one anonymous reviewer for assistance evaluating this manuscript.

References

Auriault, J. (2009), On the domain of validity of Brinkman's equation, *Transport Porous Med.*, *79*(2), 215–223.

Baldocchi, D. D., and T. P. Meyers (1998), On using eco-physiological, micrometeorological and biogeochemical theory to evaluate carbon dioxide, water vapor and gaseous deposition fluxes over vegetation, *Agric. Forest Meteorol.*, *90*, 1–26.

Battiato, I. (2012), Self-similarity in coupled Brinkman/Navier–Stokes flows, *J. Fluid Mech.*, *699*, 94–114.

Battiato, I., P. R. Bandaru, and D. M. Tartakovsky (2010), Elastic response of carbon nanotube forests to aerodynamic stresses, *Phys. Rev. Lett.*, *105*, 144504.

Breugem, W. P., B. J. Boersma, and R. E. Uittenbogaard (2006), The influence of wall permeability on turbulent channel flow, *J. Fluid Mech.*, *562*, 35–72.

Carpenter, S., and D. Lodge (1986), Effects of submersed macrophytes on ecosystem processes, *Aquat. Bot.*, *26*, 341–370.

de Langre, E. (2008), Effects of wind on plants, *Annu. Rev. Fluid Mech.*, *40*, 141–168.

Finnigan, J. (2000), Turbulence in plant canopies, *Ann. Rev. Fluid Mech.*, *32*, 519–571.

Ghisalberti, M. (2009), Obstructed shear flows: Similarities across systems and scales, *J. Fluid Mech.*, *641*, 51–61.

Ghisalberti, M., and H. Nepf (2004), The limited growth of vegetated shear layers, *Water Resour. Res.*, *40*, W07502, doi:10.1029/2003WR002776.

Ghisalberti, M., and H. Nepf (2005), Mass transport in vegetated shear flows, *Environ. Fluid Mech.*, *5*(6), 527–551.

Guo, P., A. M. Weinstein, and S. Weinbaum (2000), A hydrodynamic mechanosensory hypothesis for brush border microvilli, *Am. J. Physiol. Renal Physiol.*, *279*, F698–F712.

Hsieh, P.-C., and Y.-S. Shiu (2006), Analytical solutions for water flow passing over a vegetal area, *Adv. Water Resour.*, *29*, 1257–1266.

Jiménez, J., M. Uhlmann, A. Pinelli, and G. Kawahara (2001), Turbulent shear flow over active and passive porous surfaces, *J. Fluid Mech.*, *442*, 89–117.

Katul, G. G., D. Poggi, and L. Ridolfi (2011), A flow resistance model for assessing the impact of vegetation on flood routing mechanics, *Water Resour. Res.*, *47*, W08533, doi:10.1029/2010WR010278.

Nepf, H., and E. R. Vivoni (2000), Flow structure in depth-limited, vegetated flow, *J. Geophys. Res.*, *105*(C12), 547–557.

Nepf, H., M. Ghisalberti, B. White, and E. Murphy (2007), Retention time and dispersion associated with submerged aquatic canopies, *Water Resour. Res.*, *43*, W04422, doi:10.1029/2006WR005362.

Nepf, H. (2012), Flow and transport in regions with aquatic vegetation, *Annu. Rev. Fluid Mech.*, *44*, 123–142.

Poggi, D., C. Krug, and G. G. Katul (2009), Hydraulic resistance of submerged rigid vegetation derived from first-order closure models, *Water Resour. Res.*, *45*, W10442, doi:10.1029/2008WR007373.

Shvidchenko, A., and G. Pender (2001), Macroturbulent structure of open-channel flow over gravel beds, *Water Resour. Res.*, *37*, 709–719.

White, B., and H. Nepf (2007), Shear instability and coherent structures in shallow flow adjacent to a porous layer, *J. Fluid Mech.*, *593*, 1–32.